

Magnetic and thermodynamic properties of $\text{Li}_2\text{VOSiO}_4$: A two-dimensional $S=1/2$ frustrated antiferromagnet on a square lattice

R. Melzi, S. Aldrovandi, F. Tedoldi, and P. Carretta*

Dipartimento di Fisica "A. Volta" e Unit  INFM di Pavia, Via Bassi 6, 27100 Pavia, Italy

P. Millet

Centre d'Elaboration des Mat riaux et d'Etudes Structurales, CNRS, 31055 Toulouse Cedex, France

F. Mila

Institut de Physique Th orique, Universit  de Lausanne, CH-1015 Lausanne, Switzerland

(Received 19 December 2000; revised manuscript received 6 April 2001; published 19 June 2001)

NMR, muon spin rotation (μSR), magnetization, and specific-heat measurements in $\text{Li}_2\text{VOSiO}_4$ powders and single crystals are reported. Specific-heat and magnetization measurements evidence that $\text{Li}_2\text{VOSiO}_4$ is a frustrated two-dimensional $S=1/2$ Heisenberg antiferromagnet on a square lattice with a superexchange coupling J_1 , along the sides of the square, almost equal to J_2 , the one along the diagonal ($J_2/J_1=1.1\pm 0.1$ with $J_2+J_1=8.2\pm 1$ K). At $T_c\approx 2.8$ K a phase transition to a low-temperature collinear order is observed. T_c and the sublattice magnetization, derived from NMR and μSR , were found practically independent on the magnetic field intensity up to 9 T. The critical exponent of the sublattice magnetization was estimated $\beta\approx 0.235$, nearly coincident with the one predicted for a two-dimensional XY system on a finite size. The different magnetic properties found above and below T_c are associated with the modifications in the spin Hamiltonian arising from a structural distortion occurring just above T_c .

DOI: 10.1103/PhysRevB.64.024409

PACS number(s): 76.60.Es, 75.40.Gb, 75.10.Jm

I. INTRODUCTION

In recent years one has witnessed an extensive investigation of quantum phase transition in low-dimensional $S=1/2$ Heisenberg antiferromagnets (QHAF) as a function of doping, magnetic field, and disorder.¹ For example, two-dimensional QHAF (2DQHAF) have been widely studied in order to evidence a phase transition from the renormalized classical to the quantum disordered regime upon charge doping.² Another possibility to drive quantum phase transitions in a 2DQHAF is to induce a sizeable frustration. In particular, for a square lattice with an exchange coupling along the diagonal J_2 about half of the one along the sides of the square J_1 [see Fig. 1(a)], a crossover to a spin-liquid ground state is expected.³⁻⁵ For $J_2/J_1\leq 0.35$ N el order is realized, while for $J_2/J_1\geq 0.65$ a collinear order should develop, with spins ferromagnetically aligned either along the x axis, corresponding to a magnetic wave vector $\mathbf{Q}=(0,\pi/a)$, or along the y axis [$\mathbf{Q}=(\pi/a,0)$].⁶ Frustrated 2DQHAF are different from standard magnets mainly in two respects: first quantum fluctuations lift the degeneracy of the classical system, an effect known as order by disorder⁷ and typical of a certain class of frustrated magnets, second there is an additional Ising degree of freedom corresponding to the x - or y -collinear ground states. This twofold degeneracy can be lifted by the coupling of the spin Hamiltonian with the lattice.

Although in the last ten years an intense theoretical study of the J_2-J_1 phase diagram has been carried out a description of the temperature and magnetic-field dependence of the spin dynamics close to the critical points is still needed. Moreover, even if some frustrated 2D systems have been investigated⁸ an experimental study of the J_2-J_1 phase dia-

gram is still missing. Recently, two vanadates which can be considered as prototypes of frustrated 2DQHAF on a square lattice with $J_1\approx J_2$ have been discovered.⁹ $\text{Li}_2\text{VOSiO}_4$ and $\text{Li}_2\text{VOGeO}_4$. These two isostructural compounds are characterized by a layered structure containing V^{4+} ($S=1/2$) ions¹⁰ [see Figs. 1(b) and 2]. The structure of V^{4+} layers suggests that the superexchange couplings between first and second neighbors are similar. It is, however, difficult *a priori* to decide which one should dominate: first neighbors are connected by two superexchange channels, but they are located in pyramids looking in opposite directions and are not exactly in the same plane, whereas second neighbors are connected by one channel, but are located in pyramids looking in the same directions and are in the same plane. On the basis of NMR and susceptibility it has been possible to demonstrate that in $\text{Li}_2\text{VOSiO}_4$ J_2/J_1 is of the order of unity and that the ground state is collinear,⁹ as expected for $J_2/J_1\geq 0.65$.⁶ Moreover, from ²⁹Si NMR spectra a structural distortion occurring just above the transition to the collinear phase has been evidenced.

In this paper we present a detailed study of the magnetic and thermodynamic properties of $\text{Li}_2\text{VOSiO}_4$ by means of NMR, muon spin rotation (μSR), magnetization and specific-heat measurements. In particular, we show that the spin dynamic and static properties above the collinear ordering temperature T_c are consistent with the ones theoretically predicted for a frustrated 2DQHAF with $J_2/J_1\approx 1$. The phase transition to the collinear phase seems to be triggered by the structural distortion occurring just above T_c , which possibly modifies the superexchange couplings and lifts the degeneracy among the two ground-state configurations. The critical exponent of the sublattice magnetization and the in-

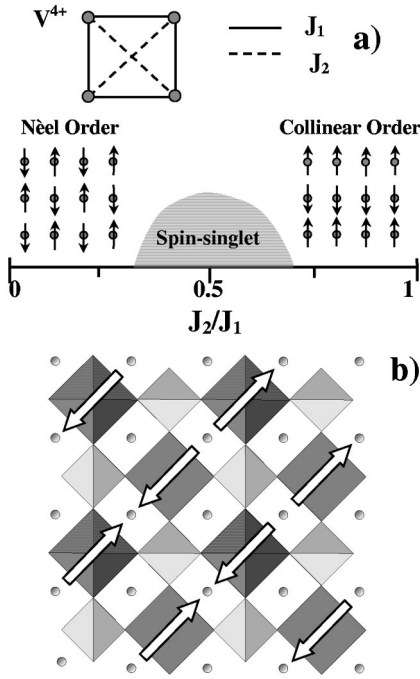


FIG. 1. (a) Schematic phase diagram of a frustrated 2DQHAF on a square lattice as a function of the ratio J_2/J_1 of the superexchange couplings. (b) Structure of $\text{Li}_2\text{VOSiO}_4$ projected along [001]. SiO_4 tetrahedra are in gray, VO_5 pyramids are in black, while the gray circles indicate Li^+ position (for details see Ref. 10). The arrows show the configuration of V^{4+} spins in the collinear ground state.

dependence of T_c on the magnetic field intensity up to 9 T, suggest that the transition is driven by the XY anisotropy.

The paper is organized as follows: in Sec. II we present the experimental results obtained by each technique; in Sec. III we discuss the experimental results in the light of numerical and analytical results for frustrated 2DQHAF on a square lattice, first for $T > T_c$ and then for $T < T_c$; the main conclusions are summarized in Sec. IV.

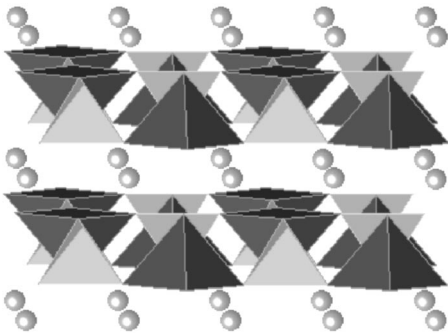


FIG. 2. Perspective view of $\text{Li}_2\text{VOSiO}_4$ showing the layered character of the structure. SiO_4 tetrahedra are in gray, VO_5 pyramids are in black, while the circles between the layers indicate Li^+ sites.

II. EXPERIMENTAL ASPECTS AND EXPERIMENTAL RESULTS

A. Sample preparation, specific heat, and magnetization

$\text{Li}_2\text{VOSiO}_4$ was prepared by solid-state reaction starting from a stoichiometric mixture of Li_2SiO_3 , V_2O_3 , and V_2O_5 according to the procedure described in Ref. 10. The sample was analyzed by x-ray powder diffraction (XRD) using a Seifert C3000 diffractometer with $\text{CuK}\alpha$ radiation and then pressed into a 1 g pellet followed by a short sintering in vacuum at 800°C for 6 h. Single crystals, of average size $1 \times 1 \times 0.2 \text{ mm}^3$, were obtained from $\text{Li}_2\text{VOSiO}_4$ powder heated at 1150°C for 2 h, slowly cooled at a rate of 5°C/h down to 1000°C and then furnace cooled down to room temperature.

Specific-heat [$C(T)$] measurements have been performed on a sintered pellet of $\text{Li}_2\text{VOSiO}_4$ by using a standard homemade adiabatic calorimeter. The contribution of the addenda decreased from about 5% to below 1% of the total heat capacity on decreasing T from 25 to 2.5 K. At low T the specific heat shows a broad maximum due to the correlated spin excitations and a sharp peak around 2.8 K [see Fig. 3(a)] associated with a second-order phase transition, as can be inferred from the nonsingular behavior of the entropy around 2.8 K. Above 20 K a rapid increase, originating from phonon excitations is observed [see Fig. 3(a)]. In order to accurately estimate the magnetic contribution $C^m(T)$ [Fig. 3(b)] to the specific heat one has to subtract the phonon term $C^p(T)$, extrapolated to low T . $C^p(T)$ was observed to follow a Debye law from 20 to 70 K, namely

$$C^p(T) = 9Nk_B \left(\frac{T}{\Theta_D} \right)^3 \int_0^{\Theta_D/T} \frac{x^4 e^x}{(e^x - 1)^2} dx, \quad (1)$$

with $\Theta_D \approx 280 \text{ K}$ the Debye temperature. It must be stressed that below 15 K $C^p(T)$ is negligible with respect to $C^m(T)$, therefore any incorrect extrapolation of $C^p(T)$ to low T will not affect the estimate of $C^m(T)$ below 15 K.

Magnetization measurements were carried out with a Quantum Design MPMS-XL7 superconducting quantum interference device (SQUID) magnetometer, both on powders and on single crystals. The T dependence of the spin susceptibility $\chi = M/H$ is shown in Fig. 4. One observes a high- T Curie-like behavior, a low T maximum around 5 K, and a kink at $T_c \approx 2.8 \text{ K}$, the same temperature where a peak in the specific heat is detected. The kink is better evidenced if one reports the derivative of the susceptibility $d\chi/dT$ (see the upper inset of Fig. 4). The susceptibility above 15 K can be appropriately fitted by

$$\chi(T) = \chi_{VV} + c_\chi / (T + \Theta), \quad (2)$$

where Θ is the Curie-Weiss temperature, $c_\chi = N_A g^2 S(S+1) \mu_B^2 / 3k_B$ (g is the Landé factor and μ_B is the Bohr magneton) is the Curie constant and χ_{VV} the Van Vleck term. The best fit of the data in the T range 10–300 K yields $\Theta = 8.2 \pm 1 \text{ K}$,¹¹ $c_\chi = 0.34 \text{ emu K/mole}$, and $\chi_{VV} = 4 \times 10^{-4} \text{ emu/mole}$. We point out that the value of c_χ is in good quantitative agreement with what one would expect for an $S = 1/2$ paramagnet, while the absolute value of χ_{VV} is

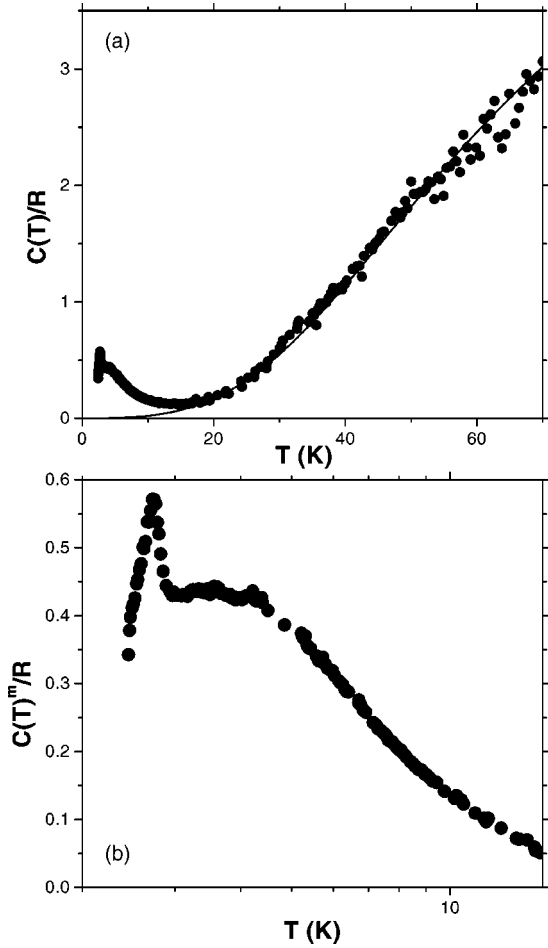


FIG. 3. (a) Temperature dependence of $\text{Li}_2\text{VOSiO}_4$ molar specific heat below 70 K. The solid lines show the phonon contribution to $C(T)$, according to Eq. (1) in the text, with $\Theta_D=280$ K. (b) Magnetic contribution to the specific heat, obtained after subtracting the phonon term corresponding to the solid line in (a).

consistent with a separation between the d_{xy} ground state and the first excited t_{2g} levels of the order of 0.15 eV, which is typical for V^{4+} in a pyramidal environment.¹² Below T_c the T dependence of the susceptibility for magnetic fields $H\parallel c$ and $H\perp c$ is different, as expected in the presence of long range order. In particular, one observes that while for $H\perp c$ the susceptibility progressively diminishes on decreasing temperature, for $H\parallel c$ it flattens (see the lower inset of Fig. 4), suggesting that V^{4+} magnetic moments lie in the ab plane.

The magnetic-field dependence of T_c , derived either from the kink in the susceptibility or from the maximum in $d\chi/dT$, was measured from 0.1 up to 7 T, where the Zeeman energy $g\mu_B H$ is greater than $k_B\Theta$, and, remarkably, T_c was not observed to vary by more than 0.07 K, i.e., less than $0.03T_c$ (see Fig. 5).

B. μSR

Zero-field (ZF) μSR measurements have been carried out on $\text{Li}_2\text{VOSiO}_4$ powders at ISIS pulsed source, both on EMU and MUSR beamlines, using spin-polarized 29 MeV/c

muons. The time evolution of the muon polarization is characterized by a constant background, due to the sample holder and cryostat walls, and by a fast decay which progressively changes from exponential to Gaussian on increasing temperature, for $T>T_c$. Below T_c both oscillating and nonoscillating components are evident (see Fig. 6), the second one with an amplitude about half of the former one, as usually expected in magnetic powders with equivalent muon sites.¹³ It must be mentioned that below T_c around 10% of the total asymmetry is missing, possibly due to fast precessing muons which cannot be detected at a pulsed muon source. Summarizing, below T_c the time evolution of the muon polarization was fitted according to

$$P_\mu(t) = A_{back} + A_1 e^{-\sigma t} \cos(\gamma B_\mu t + \phi) + A_2 e^{-\lambda t}, \quad (3)$$

where A_{back} is the sample holder background, A_1 is the amplitude of the oscillating component, with $\gamma = 2\pi \times 135.5$ MHz/T the μ^+ gyromagnetic ratio and B_μ the local field at the μ^+ , while A_2 is the amplitude of the nonoscillating component with λ the longitudinal decay rate. Above T_c the polarization was fitted by

$$P_\mu(t) = A_{back} + A e^{-\lambda t} e^{-\sigma_N^2 t^2/2}, \quad (4)$$

where the exponential term is the relaxation induced by the progressive slowing down of the V^{4+} spin fluctuations on decreasing temperature, while the Gaussian term should originate from nuclear dipolar interaction. In particular, it is likely that μ^+ localizes close to the apical oxygens, where it is coupled to ^7Li nuclear magnetic moments. The gaussian relaxation rate was estimated $\sigma_N = 0.34 \pm 0.01 \mu\text{s}^{-1}$, for $T_c \leq T \leq 4.2$ K, a value typical for relaxation driven by nuclear dipole interaction.¹³

The T dependence of the local field at the muon B_μ and of the longitudinal relaxation rate λ , derived after the fit of the data with Eqs. (3) and (4), are reported in Figs. 7(a) and 8, respectively. $B_\mu(T)$, which yields the T dependence of V^{4+} average magnetic moment, is characterized by a sharp but continuous decrease on approaching T_c , while $\lambda(T)$ is characterized by a divergence at T_c , as expected for a second-order phase transition.

C. ^7Li and ^{29}Si NMR

^7Li ($I=3/2$) NMR measurements have been carried out both on single crystals and powders, while ^{29}Si ($I=1/2$) NMR, due to the reduced sensitivity could be performed only in powder samples. The measurements have been performed using standard NMR pulse sequences. In particular, the spectra have been recorded by Fourier transform of half of the echo signal when the line was completely irradiated or by summing spectra recorded at different frequencies when it was only partially irradiated. The NMR resonance frequency of ^7Li was observed to shift to high frequencies on decreasing temperature, with a trend identical to the one of the macroscopic susceptibility (Fig. 4). In fact, for ^7Li NMR shift one can write

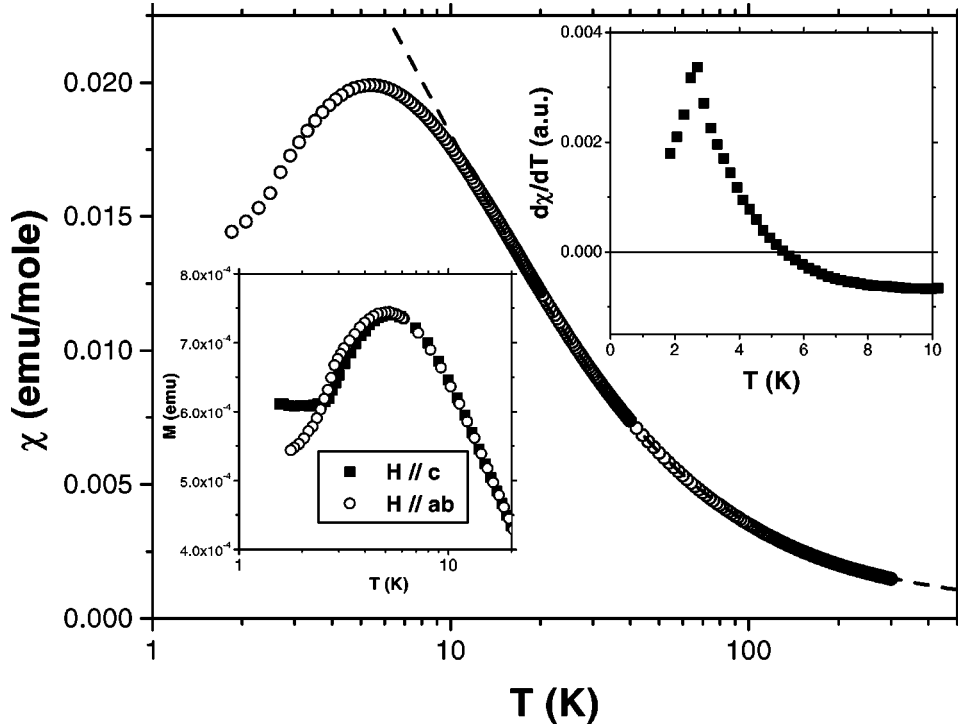


FIG. 4. Temperature dependence of the susceptibility $\chi = M/H$, for $H=3$ kG, in $\text{Li}_2\text{VOSiO}_4$ powders. The dashed line shows the best fit according to Eq. (2), for $15 \leq T \leq 300$ K. In the upper inset the derivative $d\chi/dT$ is reported, evidencing a phase transition around 2.8 K. In the lower inset magnetization measurements in a $\text{Li}_2\text{VOSiO}_4$ single crystal, both for H parallel and perpendicular to the c axis, are reported. The intensity of M for $\vec{H} \perp c$ have been rescaled for the sake of comparison.

$${}^7\Delta\mathcal{K}(T) = \frac{\sum_j \mathcal{A}_j \chi(T)}{g \mu_B N_A} + \delta, \quad (5)$$

where \mathcal{A}_j is the hyperfine coupling tensor with the j th V^{4+} and δ the chemical shift. A T dependent shift was observed both in the single crystals and in the powders, evidencing a sizeable transferred hyperfine interaction of V^{4+} spins with ${}^7\text{Li}$ nuclei. From the plot of the shift versus the susceptibility

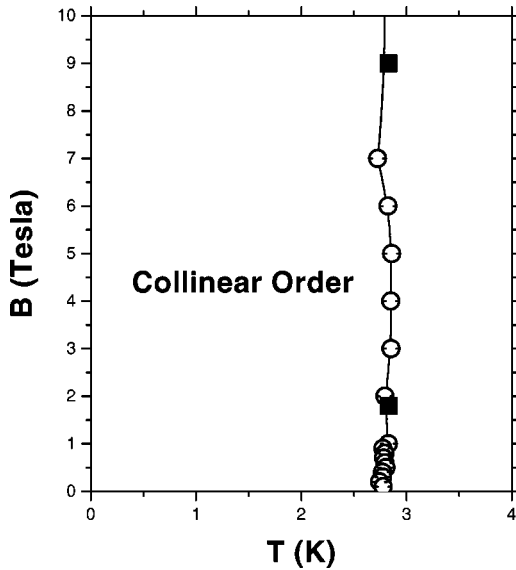


FIG. 5. Magnetic field versus T phase diagram for $\text{Li}_2\text{VOSiO}_4$. The circles indicate the field dependence of T_c derived from the kink in the susceptibility and/or from the peak in $d\chi/dT$ (see Fig. 4), while the squares indicate the corresponding values of T_c determined from ${}^7\text{Li}$ NMR spectra [see Fig. 7(b)].

(Fig. 9) the hyperfine coupling constants and the chemical shift were determined. It turns out that $\delta = -70 \pm 30$ ppm and that the hyperfine field at ${}^7\text{Li}$ is given by

$$\vec{h} = \sum_j (\mathcal{A}_{dip})_j \vec{S}_j + \sum_{i=1,2} A_i \vec{S}_i, \quad (6)$$

where \mathcal{A}_{dip} is the dipolar coupling with V^{4+} ions, while $A_i = 850$ G is the transferred coupling, which is supposed to arise from the two V^{4+} nearest neighbors only. On the other hand, ${}^{29}\text{Si}$ NMR resonance frequency in the powders is constant from room temperature down to 4 K, pointing out that the hyperfine coupling is of purely dipolar origin in this case.

Below T_c , in the single crystals, for $H \parallel c$, ${}^7\text{Li}$ NMR spectrum splits in three lines (see Fig. 10): a central one with an intensity about twice of that of two equally spaced satellites. The two satellites correspond to ${}^7\text{Li}$ sites with hyperfine fields of equal intensity but opposite orientations, while the central line corresponds to ${}^7\text{Li}$ sites where the hyperfine field cancels out.⁹ The T dependence of the satellites shift is proportional to the amplitude of V^{4+} magnetic moment and therefore it is another method, besides ZF μSR , to determine the temperature dependence of the sublattice magnetization [see Fig. 7(b)].

As already pointed out in Ref. 9, ${}^{29}\text{Si}$ NMR powder spectrum shows a quite different behavior at low T . Around 3 K, still above T_c , one observes the appearance of a shifted narrow peak. On decreasing T the low-frequency peak progressively disappears, while the intensity of the high-frequency one increases. This jump in ${}^{29}\text{Si}$ NMR shift has to be associated either with a modification of the chemical shift or of the hyperfine coupling, suggesting the occurrence of a structural distortion just above T_c . It has to be noticed that, on the contrary, no anomaly was detected in ${}^7\text{Li}$ spectra around 3

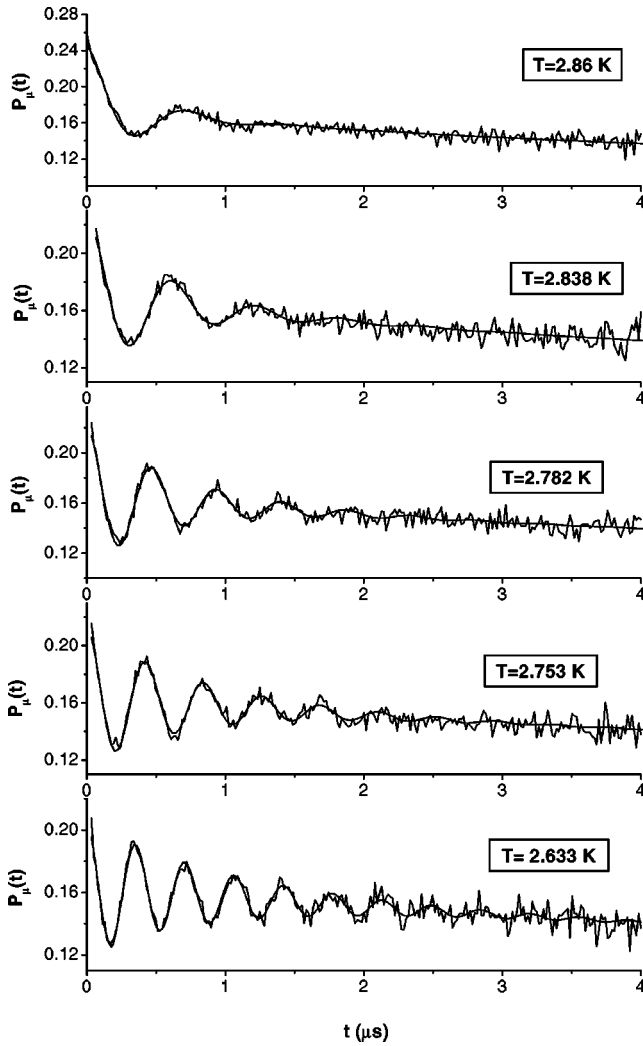


FIG. 6. Time evolution of μ^+ polarization in $\text{Li}_2\text{VOSiO}_4$ powders for T close to T_c . The solid regular line shows the best fit according to Eq. (3) in the text. The T stability was within $\pm 5 \times 10^{-3}$ K.

K. Below T_c ^{29}Si NMR linewidth is very close to the one above T_c , indicating that the local field at ^{29}Si site is zero.

The nuclear spin-lattice relaxation rate $1/T_1$ was measured by exciting the nuclear magnetization either with a comb of saturating pulses or with a 180° pulse (inversion recovery sequence). Both for ^7Li and ^{29}Si the recovery of nuclear magnetization towards equilibrium was a single exponential, indicating that for ^7Li also the $\pm 3/2 \rightarrow \pm 1/2$ lines were sizeably irradiated during the measurements. In fact, at room temperature one can discern the $\pm 3/2 \rightarrow \pm 1/2$ lines shifted by ≈ 40 kHz from the $+1/2 \rightarrow -1/2$.¹⁴ The T dependence of ^7Li $1/T_1$ is shown in Fig. 11. One observes that $1/T_1$ is constant from room temperature down to ≈ 3.2 K, then shows a peak at T_c and rapidly decreases in the ordered phase. ^{29}Si $1/T_1$ shows a similar T dependence below 4.2 K (Fig. 12); its absolute value, however, is about two orders of magnitude smaller, supporting the conclusion in favor of a hyperfine coupling of purely dipolar origin.

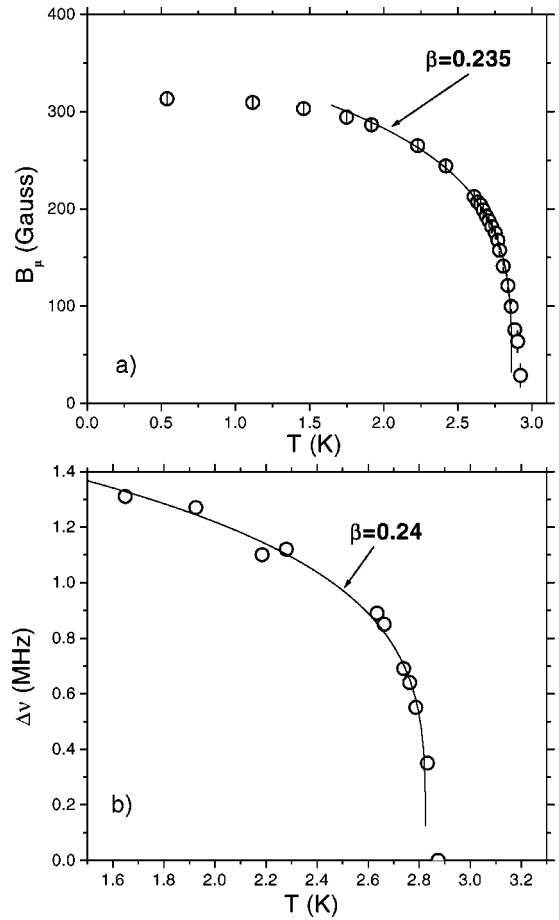


FIG. 7. (a) Temperature dependence of the local field at the muon in $\text{Li}_2\text{VOSiO}_4$ powders, derived from ZF μSR measurements. The dashed line indicates the critical behavior for a critical exponent of the magnetization $\beta = 0.235 \pm 0.009$ (see text). (b) Temperature dependence of the splitting of ^7Li NMR satellites, for $H = 1.8$ T along the c axis. The solid line shows the critical behavior for an exponent $\beta = 0.24$.

III. DISCUSSION

A. Above T_c

The T dependence of the susceptibility and of the specific heat allows us to derive information on the basic parameters of the electron-spin Hamiltonian, namely the coupling constants and their ratio J_2/J_1 . For a nonfrustrated $S = 1/2$ 2D Heisenberg AF on a square lattice the Curie-Weiss temperature $\Theta = J_1$ nearly coincides with the temperature where the susceptibility displays a maximum and one has $T_m^X = 0.935\Theta$.¹⁵ On the other hand, in $\text{Li}_2\text{VOSiO}_4$ $\Theta = J_2 + J_1 = 8.2 \pm 1$ K is significantly larger than $T_m^X = 5.35$ K (see Fig. 4), as expected for a frustrated system. By comparing the measured ratio $T_m^X/\Theta = 0.65 \pm 0.07$ with exact diagonalization and quantum Monte Carlo (QMC) results it is possible to estimate J_2/J_1 .⁹ It turns out that J_2/J_1 is close either to 0.25 or 2.5,⁹ however, it is not possible to say which of the two coupling constants is larger. We remark that these two values were estimated by assuming $\Theta = 8.2$ K, however, taking into account the uncertainty of ± 1 K in the estimate

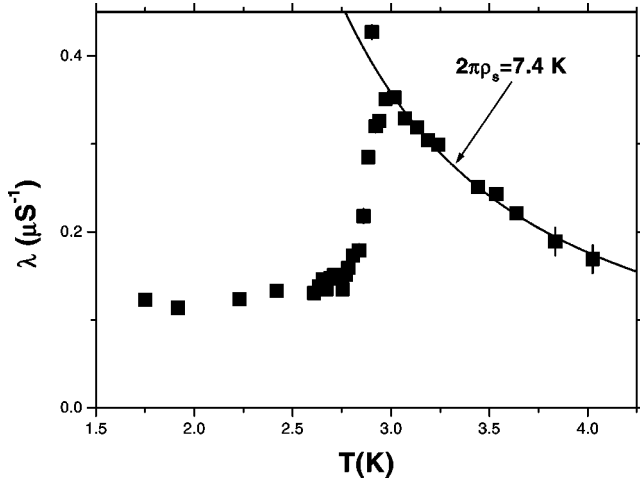


FIG. 8. Temperature dependence of the muon longitudinal relaxation rate in $\text{Li}_2\text{VOSiO}_4$ powders. The solid line indicates the T dependence of λ according to Eq. (10), with a spin stiffness $\rho_s = 7.4/2\pi$ K.

of Curie-Weiss temperature and that exact diagonalizations provide useful estimates for $J_2/J_1 < 0.4$, while QMC simulations only for $J_2/J_1 \geq 2$,⁹ it is difficult to assign an error bar to these estimates of J_2/J_1 .

A more accurate determination of the ratio J_2/J_1 can be done by analyzing $C^m(T)$ data in the light of diagonalization results by Singh and Narayanan¹⁶ and of the numerical calculations by Bacci *et al.*¹⁷ From the numerical results reported in Refs. 15 and 16 it is possible to plot the amplitude of the specific heat at the maximum $C^m(T_m^C)$ as a function of the ratio J_2/J_1 [Fig. 13(a)]. It turns out that the value $C^m(T_m^C) = (0.436 \pm 0.004)R$ found for $\text{Li}_2\text{VOSiO}_4$ ($R = N_A k_B$) (see Fig. 3) is compatible only with $J_2/J_1 = 0.44$

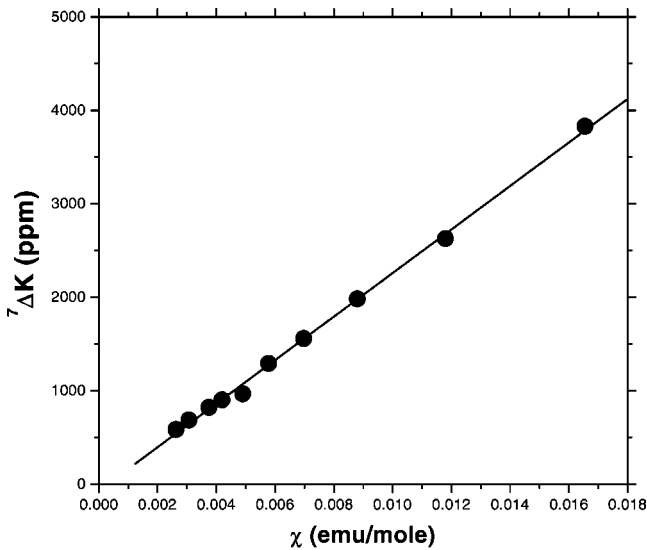


FIG. 9. Plot of ${}^7\text{Li}$ NMR paramagnetic shift versus the macroscopic susceptibility in $\text{Li}_2\text{VOSiO}_4$, for $H||c$. The solid line shows the best fit yielding a total hyperfine coupling of 2.6 kG and a chemical shift $\delta = -70 \pm 30$ ppm for $\vec{H}||c$.

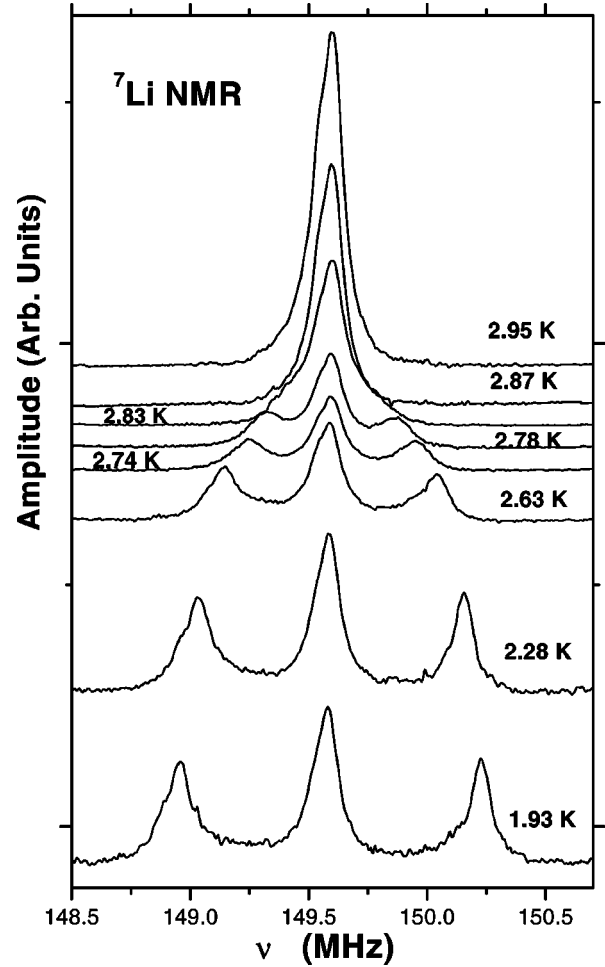


FIG. 10. ${}^7\text{Li}$ NMR spectra for $H=9$ T along the c axis in a $\text{Li}_2\text{VOSiO}_4$ single crystal, in the proximity of T_c .

± 0.01 or 1.1 ± 0.1 [Fig. 13(a)]. To discriminate among the two ratios one can analyze how $T_m^C = 3.5 \pm 0.1$ K varies as a function of J_2/J_1 . Since

$$\frac{T_m^C}{J_1} = \frac{T_m^C}{\Theta} \left(1 + \frac{J_2}{J_1} \right), \quad (7)$$

with $T_m^C/\Theta = 0.42 \pm 0.04$, one can check which value of J_2/J_1 is compatible with the results of T_m^C/J_1 vs J_2/J_1 reported by Singh and Narayanan¹⁶ [see Fig. 13(b)]. One observes that Eq. (7) is satisfied only for J_2/J_1 around 0.1 or 1.1. Therefore the only solution which is compatible with the experimental values both of T_m^C and $C(T_m^C)$ is $J_2/J_1 = 1.1 \pm 0.1$. This also indicates that Θ is close to 9 K [see Fig. 13(b)] and that $T_m^X/\Theta \approx 0.59$. Now, by assuming this value for T_m^X/Θ one would derive from the analysis of the susceptibility a value $J_2/J_1 \leq 2$, in agreement with the specific-heat analysis, even if an accurate estimate with QMC is prevented, since in this range of J_2/J_1 the results start to suffer from the minus sign problem.¹⁸ A value of J_2/J_1 around 1.1 also implies that $\text{Li}_2\text{VOSiO}_4$ lies on the right-hand side of the phase diagram reported in Fig. 1(a), where the ground

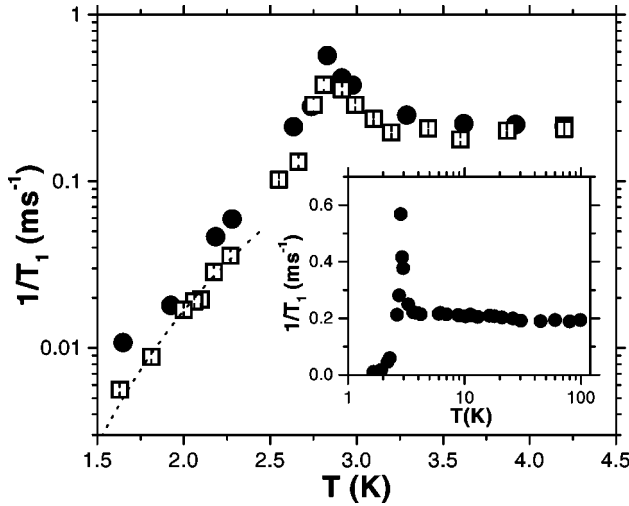


FIG. 11. ${}^7\text{Li}$ nuclear spin-lattice relaxation rate $1/T_1$ for $\vec{H}\parallel c$ in $\text{Li}_2\text{VOSiO}_4$, for $H=1.8$ T (open squares) and 9 T (closed circles). The dotted line gives the best fit according to the expression for two-magnon relaxation processes (see text), yielding $\Delta=6\pm 1$ K. In the inset the corresponding T dependence in the range 1.6–100 K is reported.

state is expected to be a collinear phase, in complete agreement with NMR results below T_c (see later on).

Further information on the superexchange constants can be achieved from the analysis of ${}^7\text{Li}$ $1/T_1$. In the limit $T \gg J_1+J_2$, $1/T_1$ is constant (see Fig. 11) and, by resorting to the usual Gaussian form for the decay of the spin-correlation function, one can write¹⁹

$$(1/T_1)_\infty = \frac{\gamma^2 S(S+1)}{2} \frac{\sqrt{2\pi}}{\omega_E} \times \sum_{k,i,j} |A_{ij}^k|^2 \quad (8)$$

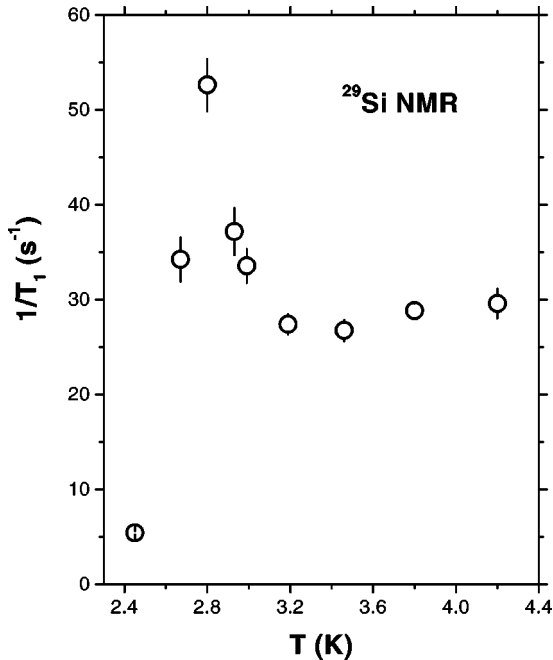


FIG. 12. ${}^{29}\text{Si}$ NMR $1/T_1$ in $\text{Li}_2\text{VOSiO}_4$ for $H=1.8$ T, for $T \leq 4.2$ K.

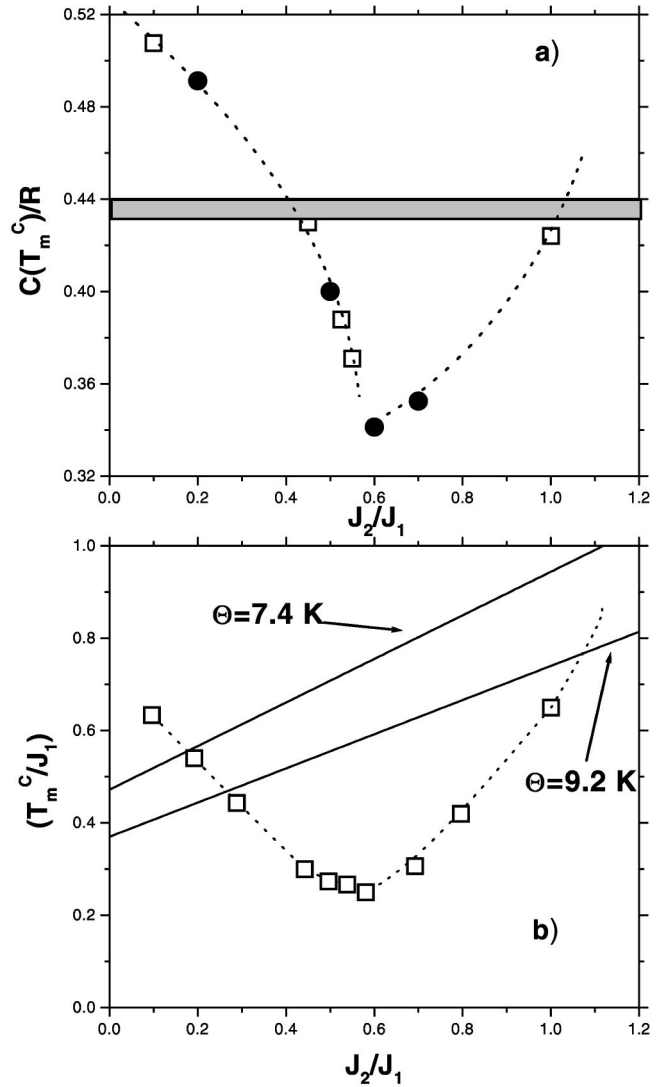


FIG. 13. (a) Amplitude of the maximum in the molar specific heat for a frustrated 2DQHAF versus J_2/J_1 . The open squares represent the data derived from Ref. 16, while the closed circles are derived from Ref. 17. The gray region around $C^m(T_m^C)/R=0.436$ represents the experimental value for this quantity, inclusive of the error bar. (b) T_m^C/J_1 (see text) versus J_2/J_1 derived from Ref. 16. The solid lines show the behavior according to Eq. (7), for values of Θ corresponding to the lower and upper limits of the Curie-Weiss temperature estimated from susceptibility measurements.

with A_{ij}^k ($i, j=x, y, z$), the components of the hyperfine tensor due to the k^{th} V^{4+} and γ the nuclear gyromagnetic ratio. $\omega_E = \sqrt{J_1^2 + J_2^2} (k_B/\hbar) \sqrt{2zS(S+1)/3}$ is the Heisenberg exchange frequency, where $z=4$ is the number of nearest-neighbor spins of a V^{4+} coupled either through J_1 or J_2 . By using in Eq. 8 $(1/T_1)_\infty = 0.2 \text{ ms}^{-1}$, i.e., ${}^7\text{Li}$ relaxation rate in the T range 300–3.2 K, one finds $\sqrt{J_1^2 + J_2^2} \approx 8.7$ K, close to what one would derive from susceptibility and specific-heat measurements.

On decreasing temperature ${}^7\text{Li}$ and ${}^{29}\text{Si}$ $1/T_1$ remain constant down to 3.2 K, at variance with μ^+ $1/T_1$ (usually called λ), which diverges on decreasing T , already at 4.2 K, due to the growth of the AF correlations. Both for nuclei and

μ^+ the spin-lattice relaxation is induced by the fluctuations of the effective local field, driven by the correlated spin dynamics, and one can write

$$1/T_1 \equiv \lambda = \frac{\gamma^2}{2N} \sum_{q,\alpha} |A_q^-|^2 S_{\alpha\alpha}(\vec{q}, \omega_R), \quad (9)$$

where $|A_q^-|^2$ is the hyperfine form factor and $S_{\alpha\alpha}(\vec{q}, \omega_R)$ ($\alpha = x, y, z$) are the components of the dynamical structure factor at the NMR or μ SR resonance frequency. One immediately realizes that a different trend of NMR and μ SR $1/T_1$ can originate from the different form factors, which couple each one of these probes in a different way with the spin excitations at the critical wave vector. In particular, one might suspect that ^7Li and ^{29}Si form factors filter out the AF correlated spin excitations. However, if one considers that ^7Li is coupled via a transferred hyperfine interaction with V^{4+} nearest neighbors [see Eq. (6)], one finds that ^7Li form factor is little \vec{q} dependent and that no filtering of the AF excitations can be envisaged. Moreover, the divergence of ^7Li and ^{29}Si $1/T_1$ at T_c evidences that the fluctuations at the critical wave vectors cannot be completely filtered out.

Another relevant difference is still present between μ SR and NMR measurements. While the former were performed in zero field, NMR $1/T_1$ measurements were carried out in magnetic fields ranging from 1.8 to 9 T, at which the Zeeman energy is comparable to the superexchange couplings. Therefore it is tempting to associate the different behavior of NMR and μ SR spin-lattice relaxation rates above T_c to a crossover of regime induced by the magnetic field. In particular, the T -independent T_1 measured in NMR would be consistent with a quantum critical regime where the in-plane correlation length $\xi(T) \propto 1/T$,²⁰ while the exponential divergence of $1/T_1$ (λ) measured with μ SR would be consistent with a renormalized classical regime where the spin stiffness ρ_s is renormalized with respect to its mean-field value by quantum fluctuations,²⁰ where, by resorting to classical scaling arguments for 2D systems, one can write²¹

$$\begin{aligned} 1/T_1(T) &\equiv \lambda(T) \propto \xi(T) \\ &= 0.493a \times e^{2\pi\rho_s/T} \left[1 - 0.43 \frac{T}{J} + O\left(\frac{T}{J}\right)^2 \right] \end{aligned} \quad (10)$$

with a the lattice step. From the T dependence of λ (see Fig. 8) above T_c one derives $2\pi\rho_s = 7.4$ K, less than the value 1.15Θ expected for a nonfrustrated system.²²

B. Below T_c

Since V^{4+} magnetic moments lie in the ab plane, as suggested by susceptibility measurements (Fig. 4) and by the EPR analysis of the g tensor,²³ and provided that the dipolar magnetic field cancels at ^{29}Si site, one realizes that the order must be collinear with a critical wave vector $\mathbf{Q} = (\pi/a, 0)$, where x is the direction of the magnetic moments.⁹

The second order transition to the low T collinear phase is evidenced by the peaks in $1/T_1$ and in $d\chi/dT$. It is remarkable to observe that T_c is practically field independent up to

at least 9 T (see Fig. 5), where $g\mu_B H/k_B > J_1 + J_2$, while a decrease is expected, with T_c vanishing for $g\mu_B H \approx 6k_B J_2$, if $J_2/J_1 = 1$, i.e., at $H \approx 20$ T.²⁴ A possible explanation for this peculiar behavior is that the structural distortion occurring just above T_c , deduced from ^{29}Si NMR spectra, causes an increase in the coupling constants and that even at 9 T $g\mu_B H/k_B < J_1 + J_2$. Another possibility is that $\text{Li}_2\text{VOSiO}_4$ is a 2D XY system with T_c close to the corresponding Berezinskii-Kosterlitz-Thouless transition.²⁴

Also the T dependence of the sublattice magnetization, derived either from the local field at the muon or from the splitting of ^7Li NMR line, was found independent on the magnetic field intensity from zero up to 9 T. From ZF μ SR measurements it has been possible to derive a critical exponent $\beta = 0.235 \pm 0.009$ for the sublattice magnetization [see Fig. 7(a)]. Remarkably, this value of β is very close to the one predicted for a 2D XY model on a finite size.²⁵ Although some in-plane anisotropy can be discerned from the susceptibility data just above T_c (see the inset to Fig. 4), there is no evidence of a crossover from Heisenberg to XY in the T dependence of the correlation length, derived from $\lambda(T)$ above T_c .²⁶ It is also interesting to observe that the sublattice magnetization measured by means of μ SR shows a slight high- T tail, as expected in a finite-size system.²⁵ If the order is purely 2D, without long-range order along the c axis, one would expect ^7Li nuclei, which lie between V^{4+} layers, to be characterized by a broad powderlike NMR spectrum. This is certainly not the case for $T_c - T \gtrsim 0.2$ K (see Fig. 10), however, one cannot exclude from the NMR measurements that the order is 2D in the very vicinity of T_c . In fact, since the strong in-plane XY correlations enhance the 3D coupling the difference between the 2D XY and 3D ordering temperatures is expected to be small, of the order of the interlayer coupling J_\perp .²⁷ An upper limit for J_\perp can be estimated by assuming that T_c is the 3D ordering temperature of a Heisenberg AF, where $T_c \approx 0.4J_\perp \xi^2(T_c)$.²⁸ From the temperature dependence of μ^+ relaxation rate λ [see Eq. (10)] one finds $\xi(T_c)/a \approx 5.3$, leading to $J_\perp \approx 0.2$ K. This value is possibly overestimated and difficult to justify if one considers the chemical bondings in the $\text{Li}_2\text{VOSiO}_4$ structure. Therefore a purely 2D order should be observable only for $T_c - T \lesssim 0.2$ K.

Although the nature of this phase transition remains to be clarified, one can argue that the insensitivity both of the Néel temperature and of the critical exponent of the sublattice magnetization to the magnetic field indicates that the phase transition is driven by the XY anisotropy.

In 3D magnets with two or more possible pitch vectors \mathbf{Q} , the ordering usually corresponds to a choice of pitch vector. The situation is often more complicated at lower temperature, and further transitions corresponding to other combinations of the pitch vectors or to the appearance of higher harmonics have been reported. Besides, the relevant parameter for the nature of the transition is the product $N = n \times m$, where n is the number of components of the order parameter (3 for Heisenberg) and m is the number of equivalent wave vectors.²⁹ As a consequence, the resulting transition can have a large critical exponent β , typically around 0.4, or might in some cases be discontinuous.

The results reported in the present paper suggest that the transition is split into two transitions: First a structural transition, as revealed by Si NMR, then an ordering transition, as seen at the Li site. A natural question arises as to whether the Ising degree of freedom corresponding to the two possible collinear states is associated with the structural distortion or with the magnetic ordering. We believe that the first possibility is the most likely both on experimental and theoretical grounds. Experimentally, the small value of the exponent β is typical of layered magnets with XY symmetry. If the parameter N was increased by a factor 2 with respect to the number of components of the order parameter due to the Ising degree of freedom, one would not expect to observe such a small exponent. Besides, the choice of a pitch vector for the collinear phase renders the two directions inequivalent, and this is likely to be coupled to the lattice and to be associated with a structural distortion.

One has to notice that the structural distortion occurring just above T_c may have modified the spin Hamiltonian. Therefore a discussion of the properties of the ordered phase on the basis of the parameters extracted above T_c could be misleading. Nevertheless, one has to notice that, to be consistent with a collinear order, J_2/J_1 must be larger than ≈ 0.65 also below T_c .

Information on the coupling constants below T_c can be derived from the T dependence of ${}^7\text{Li}$ nuclear spin-lattice relaxation. Below T_c ${}^7\text{Li}$ $1/T_1$ is mainly driven by two-magnon Raman processes,³⁰ leading to a T^3 T dependence for $T \gg \Delta$, the gap in the spin-wave spectrum, and to $1/T_1 \propto T^2 \exp(-\Delta/T)$ for $T \ll \Delta$. The low T dependence of ${}^7\text{Li}$ $1/T_1$ turns out to be activated and, by fitting the data for $T \leq 2.2$ K with the latter expression, one finds $\Delta = 6 \pm 1$ K.³¹ This value of the spin-wave gap is quite large if compared to the value of $\Theta = J_1 + J_2$, estimated from susceptibility measurements above T_c , and would imply an axial anisotropy $D \approx \Theta = 8.2 \pm 1$ K [$D \sim \Delta^2/(J_1 + J_2)$], which is quite large for V^{4+} . In fact, the values of the g factor estimated from ESR measurements are very close to 2 and yield a value of $D < 1$ K.²³ Moreover, if $D \approx \Theta$ $\text{Li}_2\text{VOSiO}_4$ should behave as an Ising system, not as an XY or Heisenberg one, in sharp contrast to the experimental findings. Thus one is tempted to argue that the low- T collinear phase is

characterized by coupling constants slightly larger than the ones determined above T_c , so that $D \ll J_1 + J_2$ and its absolute value is smaller.

Finally, one has to expect that frustration also causes a reduction of the staggered magnetization due to the enhancement of quantum fluctuations. The $T \rightarrow 0$ average magnetic moment of V^{4+} ions can be obtained from ${}^7\text{Li}$ NMR spectra below T_c . By extrapolating to $T \rightarrow 0$ the splitting of ${}^7\text{Li}$ NMR satellites and taking into account the hyperfine couplings given by Eq. (6), one can estimate a V^{4+} magnetic moment $\mu(T \rightarrow 0) \approx 0.24 \mu_B$. This value is reduced not only with respect to the value $0.65 \mu_B$ expected for a nonfrustrated 2DQHAF, but also with respect to the value derived numerically by Schulz *et al.*²² for $J_2/J_1 \approx 1$, suggesting that probably below T_c $J_2/J_1 \leq 1$.

IV. CONCLUSION

In conclusion, it has been shown that $\text{Li}_2\text{VOSiO}_4$ is a prototype of a frustrated 2DQHAF on a square lattice with $J_2/J_1 \approx 1.1$ and $J_2 + J_1 = 8.2 \pm 1$ K. Its ground state is a collinear phase, as expected for $J_2/J_1 \geq 0.65$. The phase diagram as a function of the magnetic-field intensity is characterized by a constant $T_c(H)$, for $0 \leq H \leq 9$ T. This observation, together with the fact that the critical exponent of the magnetization $\beta \approx 0.235$, suggest that the transition to the collinear phase is driven by the XY anisotropy. The structural distortion occurring just above T_c , is expected to lift the degeneracy between the two collinear ground states and to modify the superexchange couplings. In order to gain further insights on the nature of the phase transition and on the effective coupling constants below T_c further measurements with other techniques (e.g., inelastic neutron scattering) are required.

ACKNOWLEDGMENTS

A. Lascialfari and J. S. Lord are acknowledged for their help during the SQUID and μSR measurements, respectively. M. C. Mozzati is thanked for the crystal-field calculations. Fruitful discussions with L. Capriotti, A. Rigamonti, S. Sorella, and R. Vaia are gratefully acknowledged.

*Email address: carretta@fiscavolta.unipv.it

¹See, for example, E. Dagotto and T. M. Rice, *Science* **271**, 619 (1995); E. Dagotto, *Rep. Prog. Phys.* **62**, 1525 (1999), and references therein

²S. Chakravarty, B. I. Halperin, and D. R. Nelson, *Phys. Rev. B* **39**, 2344 (1989); D. Pines, *Z. Phys. B: Condens. Matter* **103**, 129 (1997).

³P. Chandra and B. Doucot, *Phys. Rev. B* **38**, 9335 (1988).

⁴H. J. Schulz and T. A. L. Ziman, *Europhys. Lett.* **18**, 355 (1992); H. J. Schulz, T. A. L. Ziman, and D. Poilblanc, *J. Phys. I* **6**, 675 (1996).

⁵S. Sorella, *Phys. Rev. Lett.* **80**, 4558 (1998); L. Capriotti and S. Sorella, *ibid.* **84**, 3173 (2000).

⁶P. Chandra, P. Coleman, and A. I. Larkin, *Phys. Rev. Lett.* **64**, 88 (1990).

⁷J. Villain, *J. Phys. (France)* **38**, 26 (1977); J. Villain *et al.*, *ibid.* **41**, 1263 (1980).

⁸Y. J. Kim *et al.*, *Phys. Rev. Lett.* **83**, 852 (1999); Y. J. Kim *et al.*, *cond-mat/0009314* (unpublished); R. Coldea, D. A. Tennant, A. M. Tsvelik, and Z. Tylczynski, *Phys. Rev. Lett.* **86**, 1335 (2001).

⁹R. Melzi *et al.*, *Phys. Rev. Lett.* **85**, 1318 (2000).

¹⁰P. Millet and C. Satto, *Mater. Res. Bull.* **33**, 1339 (1998).

¹¹The error bar of ± 1 K accounts for the systematic dependence of Θ , derived from Eq. (2), on the temperature range.

¹²Crystal-field calculations, performed taking into account the five oxygens forming V^{4+} pyramidal environment, yield the following energy splitting of the $3d$ orbitals (in eV) $E_{d_{xy}} = -0.272$, $E_{d_{xz}} = E_{d_{yz}} = -0.093$, $E_{d_{x^2-y^2}} = 0.117$, and $E_{d_{3z^2-r^2}} = 0.342$.

¹³A. Schenck, in *Muon Spin Rotation: Principles and Applications in Solid State Physics* (Hilger, Bristol, 1986).

- ¹⁴On the basis of a point-charge approximation one derives an electric-field-gradient tensor at ${}^7\text{Li}$ nuclei with its main axis tilted by $\approx 40^\circ$ from the c axis and a quadrupolar frequency of ≈ 140 kHz, yielding a shift of $\pm 1/2 \rightarrow \pm 3/2$ resonance frequency from the central resonance of ≈ 60 kHz, close to the one experimentally observed.
- ¹⁵M. Troyer (private communication).
- ¹⁶R. R. P. Singh and R. Narayanan, Phys. Rev. Lett. **65**, 1072 (1990).
- ¹⁷S. Bacci, E. Gagliano, and E. Dagotto, Phys. Rev. B **44**, 285 (1991).
- ¹⁸In most fermionic and Heisenberg spin systems, quantum Monte Carlo simulations lead to statistical weights that can be positive and negative, an effect known as the *minus sign problem*. This can lead to large statistical errors that prevent the extraction of meaningful values. For the $J_1 - J_2$ model on the square lattice, the region around $J_2/J_1 = 1/2$ is not accessible to quantum Monte Carlo for this reason. For a general discussion of the minus sign problem, see, e.g., M. Suzuki, Quantum Monte Carlo Methods in Condensed Matter Physics (World Scientific Publishing, Singapore, 1993).
- ¹⁹See H. Benner and J. P. Boucher, in *Magnetic Properties of Layered Transition Metal Compounds*, edited by L. J. de Jongh (Dodrecht, Kluwer, 1990), p. 323.
- ²⁰A. Rigamonti, F. Borsa, and P. Carretta, Rep. Prog. Phys. **61**, 1367 (1998); A. V. Chubukov, S. Sachdev, and J. Ye, Phys. Rev. B **49**, 11 919 (1994).
- ²¹P. Carretta *et al.*, Phys. Rev. Lett. **84**, 366 (2000).
- ²²H. J. Schulz, T. A. L. Ziman, and D. Poilblanc, J. Phys. I **6**, 675 (1996).
- ²³V. Pashchenko, Y. Ksari, and A. Stepanov (unpublished).
- ²⁴See H. J. M. de Groot and L. J. de Jongh, in *Magnetic Properties of Layered Transition Metal Compounds*, edited by L. J. de Jongh (Dodrecht, Kluwer, 1990), p. 379; see also M. E. Zhitomirsky, A. Honecker, and O. A. Petrenko, Phys. Rev. Lett. **85**, 3269 (2000).
- ²⁵S. T. Bramwell and P. C. W. Holdsworth, Phys. Rev. B **49**, 8811 (1994); S. T. Bramwell and P. C. W. Holdsworth, J. Phys.: Condens. Matter **5**, L53 (1993).
- ²⁶B. J. Suh *et al.*, Phys. Rev. Lett. **75**, 2212 (1995).
- ²⁷H.-Q. Ding, Phys. Rev. Lett. **68**, 1927 (1992).
- ²⁸D. C. Johnston, in *Handbook of Magnetic Materials*, edited by K. H. J. Buschow (Amsterdam, North Holland, 1997), Vol. 10, Chap 1, p. 1.
- ²⁹See, e.g., the discussion in J. Jensen and A. R. Mackintosh, *Rare Earth Magnetism* (Oxford Science Publications, New York, 1991), and references therein.
- ³⁰D. Beeman and P. Pincus, Phys. Rev. **166**, 359 (1968).
- ³¹This value of Δ is reduced with respect to the value ($\Delta \approx 18$ K) previously reported in Ref. 9. The reason is that in Ref. 9 $1/T_1$ has been fitted with a simple Arrhenius law, without the T^2 prefactor, and over a T range limited to higher temperatures.